Design and Application of a Two Pole Spherical Permanent Magnet Motor

Sibel Akkaya Oy [1], Osman Gürdal [2]

[1]*Fatsa Faculty of Marine Sciences, Ordu University,Ordu,52400 Turkey*

[2] *Faculty of Technology, Gazi University, Ankara, Turkey*

***Abstract*—In this study, an air core spherical motor comprising a two pole permanent magnet rotor with 8 mm diameter and a multipole stator is designed by considering the ease of manufacturing priorities. Stator winding dimensions are calculated in a way to give maximum torque to the rotor analytically. Magnetic field distribution and torque values are calculated analytically. Stator coils in the yoke made from Delrin are positioned in proper values. Spherical motor with three poles stator and two poles rotor can move 44° up and down in 360° azimuthal angles without direct rotational movement in an open loop system and it is suitable to use in cascade in a robotic system.**

***Keywords*— Spherical Motor; Permanent Magnet; Geodesic Arc Length; Torque.**

1. Introduction

In the industrialized world today, many systems used from manufacturing to the other sub-sectors are shifting to robotic applications via automation systems. Due to these developing and rapidly growing technologies, a trend in which robotic applications show progress has formed. In order to meet these needs of the industry, actuators used in these robotic systems are needed to be designed according to the needs. Designing spherical motors that can rotate with 2 and 3 degrees of freedom offers great advantages in this field. The major advantages of spherical motors are fast reaction times, high efficiencies and having high precision motion [1,2].

DOI: 10.18421/TEM71-07
https://dx.doi.org/10.18421/TEM71-07

Corresponding author: Sibel Akkaya Oy,
Fatsa Faculty of Marine Sciences, Ordu University, Ordu, Turkey
Email: sibelakkayaoy@gmail.com

Received: 21 December 2017.
Accepted: 03 February 2018.
Published: 23 February 2018.

When the development of spherical motors in time is investigated, Williams and Laithwaite's study on induction motors with various speeds in 1950s has enabled induction motor to be developed with spherical geometry [3]. Based on Williams and Laithwaite's studies, Vachtsevanos et al. designed a spherical motor with 3 degrees of freedom [4]. Then they performed electromagnetic analysis of this motor by using ideal distributed current model [5]. Kaneko et al. developed a spherical DC servo motor that can move with three degrees of freedom [6]. This rotor assembly is performed around the center shaft. Because of the limited movement area of a DC spherical motor and complex mechanical structure of spherical induction motor and its manufacturing difficulties, Lee et al. introduced a spherical step motor concept and designed a variable spherical step motor taking the step motor as basis [7,8]. Lee et al. introduced a dynamic model of a spherical motor with varying reluctance in terms of torque model and rotor dynamics [9]. In order to place more than twenty poles equally onto the semi spherical stator, Lee and Kwan developed a program and designed the rotor poles with two permanent magnets to provide three degrees of freedom movement [10]. Lee and Kwan also developed a theory based on local interaction between the rotor and the stator which are close to each other. By analyzing the kinematic relationship between the rotor and the stator poles close to each other, Lee et al. stated that several equally spaced stator poles are required for motion control [11]. Lee and Kwan suggested that the sustainability model is an important concept in order to predict the torque produced by the variable reluctance spherical motor [10]. On this concept, Pei made more theoretical research and Roth and Lee explained this model experimentally [12,13]. Bai et al. presented a new method, referred here as back-EMF method, for sensing the multi-DOF motion of a permanent magnet spherical motor [14].

In this study, an air core spherical motor is designed. The rotor of the spherical motor is a two poles NdFeB permanent magnet. The stator is composed of three coils. The study is mostly focused on determining particularly the stator conical coil angles analytically. In order to determine $\zeta 0$ and $\zeta 1$ angles determining the optimum geometrical shape of the coils, an equation is defined. To create the

torque model of the designed motor, torque calculations are performed.

2. Magnetic field distribution

Magnetic field distribution generated by the permanent magnet in spherical motor design forms the basis in the motor design optimization and developing the control section [3]. Magnetic field is divided into two zones. The first one is the air gap outside the rotor. The second one is the poles of the permanent magnet.

Magnetic flux density in the air gap outside the rotor [3]:

$$B = \mu_o H_I \quad (1)$$

where μo is the magnetic permeability of the air, B is the magnetic flux density and H is the magnetic field strength. Magnetic flux density in the permanent magnet poles is [3]:

$$B = \mu_o \mu_r H_{II} + \mu_o M_o \quad (2)$$

where, μr is the relative permeability of the magnet. $M_o = \frac{B_{rem}}{\mu_o}$ is the permanent magnetization. For the magnetic field,

$$\nabla \times H = 0 \quad (3)$$

Magnetic field strength is defined as the gradient of scalar potential of Φ and shown as in Eq. (4).

$$H = -\nabla \Phi \quad (4)$$

As a result of the implementation of Laplace equation, the following field equations are obtained [14].

In permanent magnet;

$$\nabla^2 \Phi_{ii} = (\nabla . M_o)/\mu_r \quad (5)$$

In air;

$$\nabla^2 \Phi_I = 0 \quad (6)$$

The radial component of the magnetization vector is expressed now as follows [14].

$$M_{0r} = (-1)^{P-1} M_o \cos\left[\phi - \alpha_o - \frac{2\pi}{P}(p-1)\right] \sin\theta \quad (7)$$

where p is the total pole number of the permanent magnet. Magnetic flux density in the air gap zone can be expressed as follows by considering the boundary conditions.

$$B_{Ir} = -\mu_o \frac{d\Phi_I}{dr} \quad (8)$$

where the scalar potential is [14]:

$$\Phi_I = \xi_{nl}^m r^{-(n+1)} \left\{Y_n^m(\theta,\phi)\right\} + \xi_{nl}^{-m} r^{-(n+1)} \left\{Y_n^{-m}(\theta,\phi)\right\} \quad (9)$$

$Y_n^m(\theta,\phi)$where the spherical harmonic function [14] and defined as follows.

$$Y_n^m(\theta,\phi) = \sqrt{\frac{2n+1}{4\pi}\frac{(n-m)!}{(n+m)!}}[P_n^m(\cos\theta)]e^{im\phi} \quad (10)$$

where $P_n^m(\cos\theta)$ shows the mth degree Legendre function in nth row and $-n \le m \le n$ while n and m are integers. ξ_{nI}^m Expression in Eq. (9) is a constant which will be determined by the boundary conditions [13] The boundary conditions are as follows. Expansion of the coefficient ξ_{nI}^m is given in Eq. (12).

$$\begin{aligned} &B_{Ir}|r = R_o = B_{IIr}|r = R_o \\ &H_{I\phi}|r = R_o = H_{II\phi}|r = R_o \quad \text{and} \\ &H_{I\theta}|r = R_o = H_{II\theta}|r = R_o \end{aligned} \quad (11)$$

$$\xi_{nI}^m = C_{n,m} d_n \qquad \xi_{nI}^{-m} = C_{n,-m} d_n \quad (12)$$

where $dn = -d_n^1/d_n^2$.

Cnm is determined by the surface integral, as shown below [14].

$$C_{nm} = M_o \int_0^{2\pi} f(\phi)]e^{-im\phi} d\phi \int_0^{\pi} \sqrt{\frac{2n+1}{4\pi}\frac{(n-m)!}{(n+m)!}}[P_n^m]e^{im\phi} \sin^2\theta d\theta \quad (13)$$

where

$$f(\phi) = (-1)^{P-1} cos\left[\phi - \alpha^0 - \frac{\pi}{4}(p-1)\right] d\phi \quad (14)$$

$$a \pm bi \equiv \int_0^{2\pi} f(\phi)]e^{-im\phi} d\phi \quad (15)$$

where the boundary conditions of ϕ are $\frac{\pi}{4}(p-1) + \alpha^0 - \frac{\alpha}{2} < \phi < \frac{\pi}{4}(p-1) + \alpha^0 + \frac{\alpha}{2}$. The value a is not seen to be 0 in the values of m=0, ±4, ±8, ±12, ±16,……..

$$c/\sqrt{\pi} \equiv \int_0^{\pi} \sqrt{\frac{2n+1}{4\pi}\frac{(n-m)!}{(n+m)!}}[P_n^m(\cos\theta)]e^{im\phi} \sin^2\theta d\theta \quad (16)$$

where the boundary conditions of θ are $\frac{\pi}{2} - \frac{\beta}{2} < \theta < \frac{\pi}{2} + \frac{\beta}{2}$. For the values of n= ±2, ±4, ±6, …….., the result of $c \neq 0$ is found. For odd numbers $c = 0$. Wherein, a, b and c are real numbers.

3. Torque model

While the torque model is designed, Lorentz force law is utilized. Due to the interaction between the rotor magnetic field and the stator windings in which a current flows, a torque is generated on the rotor [3].

$$T = -\int_v r \times (J \times B) dv \quad (17)$$

where J is the current density.

If it is integrated over the whole coil volume, the torque equation can be written as below. The symbol c represents the circular loop in the winding [14].

$$T_c = -J \int_{R_1}^{R_2} \int_{\zeta_0}^{\zeta_1} \{\int_c r B_{Ir}(r, \theta, \phi) dl\} r dr d\zeta \quad (18)$$

If the torque produced by ith winding is named as Ti , θi and ϕi represent the axis position of the winding. R1 is the distance between the inner surface of the winding and the center, R2 is the distance from the outer surface of the winding to the center, ζ0 is the angular diameter of the air core, ζ1 is the angular diameter of the windings. Output torque in a single coil is expressed as the following equation [15].

$$T_i = T_c G(\theta_i, \phi_i) J_i \quad (19)$$

where:

$$T_i = [T_{ix}, T_{iy}, T_{iz}]^T$$

where,

$$G(\theta_i, \phi_i) = [g_x(\theta_i, \phi_i), g_y(\theta_i, \phi_i), g_z(\theta_i, \phi_i)]^T$$

$$T = T_c \begin{bmatrix} g_x(\theta_1, \phi_1) g_x(\theta_2, \phi_2) \ldots\ldots g_x(\theta_N, \phi_N) \\ g_y(\theta_1, \phi_1) g_y(\theta_2, \phi_2) \ldots\ldots g_y(\theta_N, \phi_N) \\ g_z(\theta_1, \phi_1) g_z(\theta_2, \phi_2) \ldots\ldots g_z(\theta_N, \phi_N) \end{bmatrix} \begin{bmatrix} J_1 \\ J_2 \\ J_N \end{bmatrix} \quad (20)$$

4. Prototype development

Since the spherical motor in this performed design has an air core, stator part of the designed spherical motor is made by Delrin material. Stator poles are placed with a 45° angle to the x axis and with a 120° angle to the z axis. There is a 0.1 mm air gap between the stator poles and rotor poles.

The properties of this prototype are shown in Table 1.

Table 1. The properties of this prototype

Stator radius	5.7 (mm)
Rotor radius	4 (mm)
Polar angle of the permanent magnet	α=180°, =90°
The number of stator poles	3
The number of rotor poles	2
Maximum tilt angle	± 44
Maximum torque	30 (uNm)

In Figure 1, simple structure of the motor on the drawing editor in Ansoft Maxwell 3D can be seen. A prototype of the spherical motor designed is shown in Figure 2. There are three stator poles and each has three coils (coil1, coil 2 and coil 3). These coils generate electromagnetic forces along the stator. The rotor of the motor also has two poles.

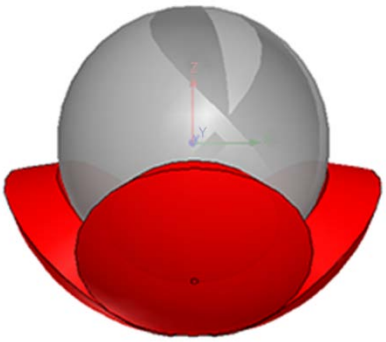

Figure 1. Basic structure of the motor

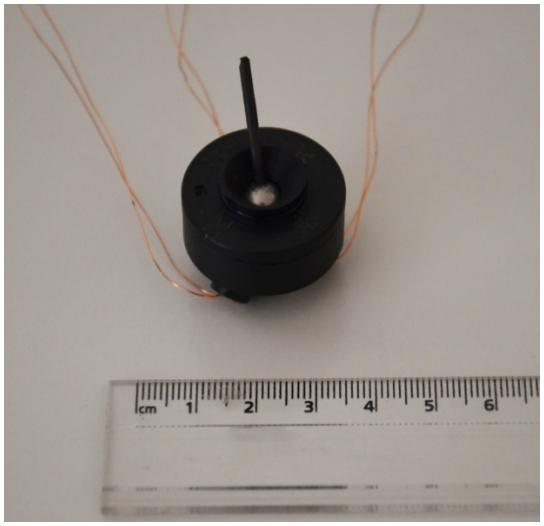

(a)

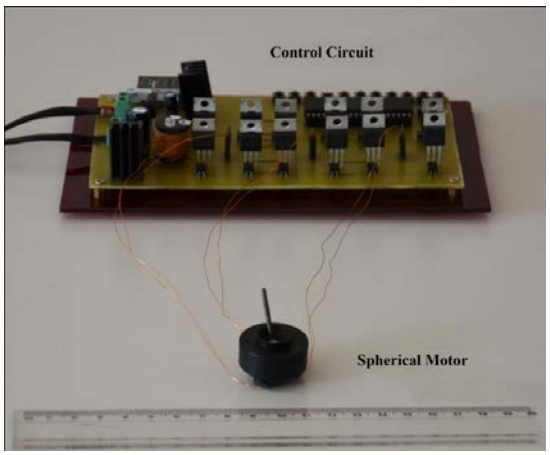

(b)

Figure 2. Spherical motor prototype: (a) The prototype of motor, (b) Spherical motor control circuit

The magnetic circuit would be short according to the minimum reluctance principle. The flux density of the motor is shown in Figure 3. The directions of the magnetic flux density are as shown in the Figure 3 (a), the stator is straight from the rotor.

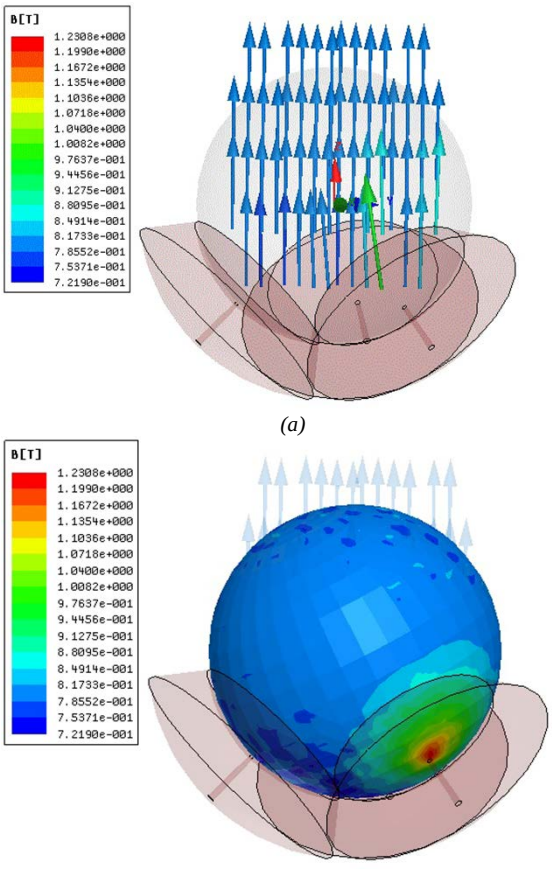

(a)

(b)

Figure 3. The flux density of the motor: (a) Vector representation, (b) Magnetic representation

Determination of coil conical angle

Maximum torque (Tm) is related with the conical angles of stator windings (ζ0 - ζ1) and the start and end radii of the windings (r1-r2). Since D is a multiplier in torque equation, the maximum value of the torque can be calculated with the second derivative of D in terms of ζ0 and ζ1. D is expressed as in the following equation [3].

$$D = \pi B_{rem} J \left\{ \zeta_1 - \zeta_0 + 0.5\left(\sin 2\zeta_0 - \sin 2\zeta_1\right) \right\} \quad (21)$$

By keeping ζ0 constant, the first and the second derivatives of D are taken as shown below.

$$D'_{\zeta_1} = \left(1 - \zeta_0 + \frac{\sin 2\zeta_0}{2} - \cos 2\zeta_1\right) \quad (22)$$

$$D''_{\zeta_1} = \left(-\zeta_0 + \frac{\sin 2\zeta_0}{2} + 2\sin 2\zeta_1\right) \quad (23)$$

The graphs drawn according to the above equations are given in Figure 4. and Figure 5. For the maximum torque, ζ0 and ζ1 must be ζ0=0° and ζ1= π/2. Since ζ0=0 is not possible, ζ0 should be kept as small as possible. Because of the physical conditions it is taken as ζ0=7°

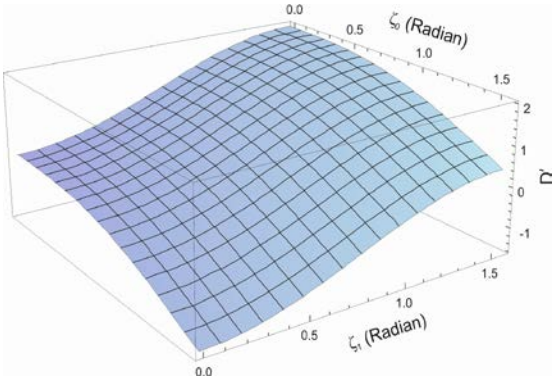

Figure 4. $D''_{\zeta 1}$ graph

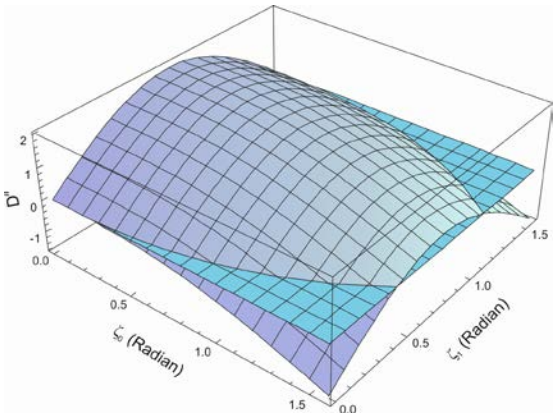

Figure 5. $D''_{\zeta 1}$ graph

Since ζ1= π/2 is not possible, to find the value of ζ1 angle which can generate maximum torque, geodesic arc length formulas are used in spherical coordinate system. In the spherical coordinate system;

$$r\vec{a}_{r_i} = r\sin\theta_i\cos\varphi_i\,\vec{a}_x + r\sin\theta_i\sin\varphi_i\,\vec{a}_y + r\cos\theta_i\,\vec{a}_z \quad (24)$$

To find the angle (φ) between two radial vectors as i=1,2 in radius r defined as above, dot product is

used.

$$
\begin{aligned}
&(r\,\vec{a}_{r_1})\cdot(r\,\vec{a}_{r_2})\\
&=\\
&(r\sin\theta_1\cos\phi_1\,\vec{a}_x + r\sin\theta_1\sin\phi_1\,\vec{a}_y +\\
&r\cos\theta_1\,\vec{a}_z)\cdot(r\sin\theta_2\cos\phi_2\,\vec{a}_x +\\
&r\sin\theta_2\sin\phi_2\,\vec{a}_y + r\cos\theta_2\,\vec{a}_z)\\
&=\\
&r^2\cos\varphi = r^2(\sin\theta_1\cos\phi_1\sin\theta_2\cos\phi_2 +\\
&\sin\theta_1\sin\phi_1\sin\theta_2\sin\phi_2 + \cos\theta_1\cos\theta_2)\\
&=\\
&r^2[\sin\theta_1\sin\theta_2\underbrace{(\cos\phi_1\cos\phi_2 + \sin\phi_1\sin\phi_2)}_{\cos(\phi_1-\phi_2)} +\\
&\cos\theta_1\cos\theta_2]\\
&=\\
&r^2\underbrace{[\sin\theta_1\sin\theta_2\cos(\phi_1-\phi_2) + \cos\theta_1\cos\theta_2]}_{\cos\varphi}
\end{aligned}
\tag{25}
$$

A a result of the above equation, arc length (s) can be found as below:

$$s = r\ = r\cos^{-1}[\sin\theta_1\sin\theta_2\cos(\varphi_1-\varphi_2)+\cos\theta_1\cos\theta_2] \tag{26}$$

Arc lengths for three coils are found by using the above equation. This found arc length also gives ζ1 angle necessary to produce maximum torque in three windings.

$$
\begin{aligned}
&s_3 = 4\cos^{-1}[\cos 45°\cos 45° +\\
&\sin 45°\sin 45°\cos(0°-120°)] = 5{,}27246\\
&\frac{5{,}27246}{4\pi}180° = 75{,}52242641°
\end{aligned}
\tag{27}
$$

where $\zeta_1 = 37{,}76121321°$. Because of the physical conditions it is taken as ζ1=37°.
S changes depending on the coil angles of ζ0 and ζ1 and S is given as an equation below.

$$S = -{}^{4}/_{3}(\sin^3\zeta_1 - \sin^3\zeta_0) + {}^{7}/_{5}(\sin^5\zeta_1 - \sin^5\zeta_0) \tag{28}$$

S value in Eq. (28) changes the torque output. Accordingly, how the coil conical angles we will use in this motor design will change the torque output can be seen in the graphs. In Figure 6, how S value and thus the torque output decrease with the increase of ζ0 angle can be seen. In Figure 7, how S value and thus the torque output increase with the increase of ζ1 angle can be seen.

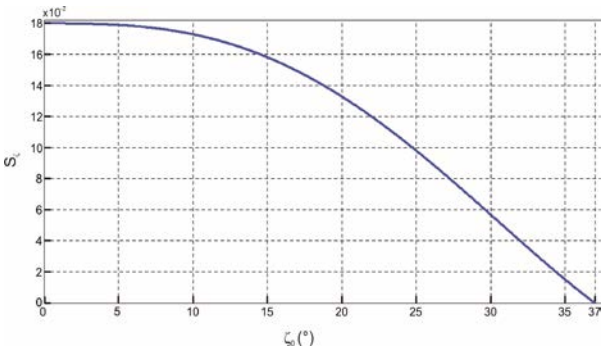

Figure 6. Coil parameter ζ0 vs Sζ (ζ1= 37°)

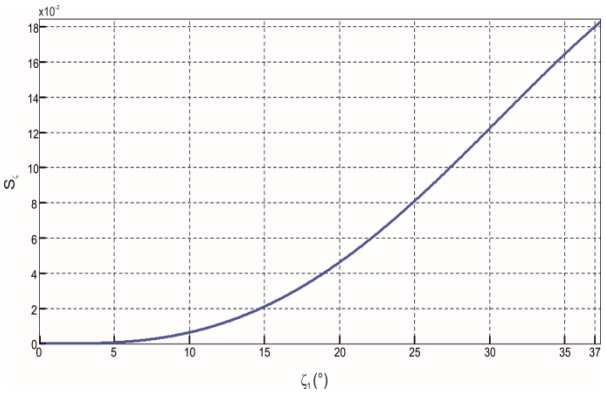

Figure 7. Coil parameter ζ1 vs Sζ (ζ0=0°)

Solving the torque integral

For *n*=4, *m*=4, torque calculation is made by using the above equations. Where *p* is taken as *p*=2. For *n* and *m* values, $a = -\frac{2}{15}$, $b = 0$, $c = \frac{42\sqrt{35}}{32\sqrt{2}}\pi$, $Y_4^4(\theta,\phi) = \frac{3}{8}\sqrt{\frac{35}{8\pi}}sin^4\theta e^{4i\phi}$ are found. When the values are substituted in Eq.(8). $B_{Ir(4,4)} = -\frac{735}{256}M_0 d_4 r^{-6} sin^4\theta cos4\phi$ is found. Substituting these obtained results in Eq. (18):

$$T_i = -\frac{735}{256}J\mu_0 M_0 d_4 R_c \int_{\zeta_0}^{\zeta_1}\left\{\int_0^{2\pi}\sin^4\theta\cos 4\phi r\sin\zeta d\psi .\left(\cos\psi\, e_{\phi i} - \sin\psi\, e_{\theta i}\right)\right\}d\zeta \tag{29}$$

can be written. Where, $R_c = R_2^{-2} - R_1^{-2}$ dir. $d_4 = \frac{R_0^6}{(4\mu_r+5)}$. The expression in the integral can be defined as *D* (*θ*, *ϕ*) [14]. The integrated version of this expression will become as follows [14].

$$D^e(\theta,\varphi) = \pi\sin^3\theta\left(-4/3\sin^3\zeta + 7/5\sin^5\zeta\right)\left[\cos\theta\cos 4\varphi\, e_\varphi + \sin 4\varphi\, e_\theta\right] \tag{30}$$

$$S\zeta = -{}^{4}/_{3}\left(sin^3\zeta_1 - sin^3\zeta_0\right) + {}^{7}/_{5}\left(sin^5\zeta_1 - sin^5\zeta_0\right) \tag{31}$$

$$D_c^e(\theta_i,\varphi_i)=\pi S\left(\sin^3\theta\cos\theta\sin 3\varphi e_x+\sin^3\theta\cos\theta\cos 3\varphi e_y - \sin^4\theta\sin 4\varphi e_z\right) \quad (32)$$

$$T_I=\begin{bmatrix}T_x\\T_y\\T_z\end{bmatrix}=T_c\begin{bmatrix}sin^3\theta cos\theta sin3\phi\\sin^3\theta cos\theta cos3\phi\\-sin^4\theta sin4\phi\end{bmatrix}J \quad (33)$$

where the expression T_c is given as an equation below [14].

$$T_c=-{}^{735}/_{512}J\mu_o M_0 d_4 R_c S\pi \quad (34)$$

In Figure 8, with analytical and simulation results for the rotor when ϕ=0°, θ=0° and θ=44° are compared.

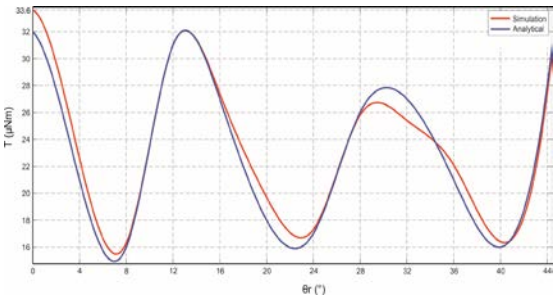

Figure 8. Torque vs. θr

Torque value measured as a result of the application is approximately 30 μNm. In the calculations, these values of μ_o=4π10^{-7} H/m, μ_r=1,099 H/m, B_{rem}=1,23 T are considered.

5. Conclusions

In this study, an air core spherical motor composed of two poles permanent magnet rotor and multipole stator is optimized and designed by considering the production ease. Magnetic field distribution generated by the rotor poles of the spherical motor and the torque model of the spherical motor are expressed. Another important factor affecting the output torque is the coil conical angle determining the coil geometry. Coil conical angle of the designed stator windings are found in a way to obtain maximum torque with analytical calculation by using the geodesic arc length formulas by considering the ideal and physical limitations which is the first approach in the literature.

References

[1] Gürdal, O. & Öner, Y. (2005). Three Dimensional Magnetostatic Analysis and Application of Iron Cored Permanent Magnet Spherical Actuator. *J. Fac. Eng. Arch. Gazi Univ.*, 20, 433-442.

[2] Öner, Y. (2007). A permanent magnet spherical rotor design and three dimensional static magnetic analysis. *Sensors and Actuators A: Physical*, *137*(2), 200-208.

[3] Wang, J., Jewell, G.W., Howe, D. (1998). Analysis, design and control of a novel spherical permanent-magnet actuator. *Electric Power Applications, IEE Proceedings*, *145*(1), 61-71.

[4] Vachtsevanos, G., Davey, K., & Lee, K. M. (1987). Development of a novel intelligent robotic manipulator. *IEEE Control Systems Magazine*, *7*(3), 9-15.

[5] Davey, K., Vachtsevanos, G. & Power, R. (1987). The analysis of fields and torques in spherical induction motors. *IEEE Transactions on Magnetics*, *23*(1), 273-282.

[6] Kaneko, K., Yamada, I., & Itao, K. (1989). A spherical DC servo motor with three degrees of freedom. *Journal of dynamic systems, measurement, and control*, *111*(3), 398-402.

[7] Lee, K. M., Vachtsevanos, G., & Kwan, C. K. (1988, April). Development of a spherical wrist stepper motor. In *Proceedings of the 1988 IEEE lntemational Conference on Robotics and Automation, Philadelphia, PA. April* (pp. 26-29).

[8] Lee, K. M., Pei, J., & Roth, R. (1994). Kinematic analysis of a three-degrees-of-freedom spherical wrist actuator. *Mechatronics*, *4*(6), 581-605.

[9] Lee, K.M., Wang, X. & Wang, N.H. (1993). Dynamic modeling and control of a ball-joint-like variable-reluctance spherical motor. *Symposium on Mechatronics*, *ASME Winter Annual Meeting*, New Orleans, 71-79.

[10] Lee, K.M. & Kwan, C.E. (1991). Design concept development of a spherical stepper for robotic applications. *IEEE Transactiona on Robotics and Automation*, *7*(1), 175-181.

[11] Lee, K. M., Pei, J., & Roth, R. (1994). Kinematic analysis of a three-degrees-of-freedom spherical wrist actuator. *Mechatronics*, *4*(6), 581-605.

[12] Pei, J. (1990). *Methodology of design and analysis of variable-relüktance spherical motors*. Ph.D. thesis, Dept. Mechanical engineering, Georgia Tech, USA.

[13] Roth, R. & Lee, K.M. (1995). Design optimisation of a three degrees of freedom variable reluctance spherical wrist motor. *Transcations of the ASME Journal of Engineering for Industry*, *117*(3), 378-388.

[14] Yan, L., Chen, I. M., Lim, C. K., Yang, G. & Lee, K. M. (2011*). Design, Modeling and Experiments of 3-DOF Electromagnetic Spherical Actuators*. Mechanisms and Machine 4, Springer Science+Business Media B. V., 32-53.

[15] Yan, L., Chen, I. M., Lim, C. K., Yang, G., Lin, W., & Lee, K. M. (2008). Design and analysis of a permanent magnet spherical actuator. *IEEE/ASME Transactions on mechatronics*, *13*(2), 239-248.